ACTA GEOGRAPHICA LODZIENSIA
118 (2025): 91-106
https://doi.org/10.26485/AGL/2025/118/6

# SPATIOTEMPORAL DYNAMICS AND PREDICTION OF LAND USE AND LAND COVER CHANGES UNDER SEISMIC HAZARD: A CASE STUDY OF THE ORAN REGION, ALGERIA

FARID RAHAL[1]*, FATIMA-ZOHRA BABA-HAMED[2]

**Abstract.** Seismic hazard cannot be understood solely as an exogenous threat. It is part of a broader urban dynamic. The city of Oran is a telling example, its expansion being highlighted through the study of land use and land cover (LULC) trends based on a time series of Landsat satellite images from 2015 to 2025 with a five-year interval.

Over the past 15 years, the study area has experienced a significant increase in built-up area, increasing from 9.59% to 13.83%, while vegetation cover has decreased from 21.65% to 16.56%.

Furthermore, predictions (2030–90) confirm the growing trend towards artificialization of surfaces.

The relationship between urban growth and seismic hazard is important to examine. Indeed, the overlay of maps of predicted urban growth and those of seismic wave amplification zones showed that there will be a sharp increase in the level of urbanization in areas representing a medium seismic hazard.

**Key words:** LULC, Modeling, Prediction, Seismic hazard, Artificialized surfaces

## Introduction

Land use and land cover (LULC) analysis based on satellite imagery allows for the monitoring of land use and land cover changes over time and space, with broad coverage and regular access (Lu *et al.* 2007; Roy *et al.* 2014).

Furthermore, satellite data provide long time series that are generally cost-free to access, making them ideal for historical analysis, as is the case with data from Landsat missions launched since 1972 (Charnell *et al.* 1973; Cohen *et al.* 2004). This is also the case for the Sentinel family of satellites, the first of which was launched in 2014 (Drusch *et al.* 2012; Sun *et al.* 2019).

The study of LULC dynamics supports urban planning, natural resource management and policies aimed at achieving environmental sustainability (Verburg *et al.* 2013). This technique makes it possible to monitor environmental impacts by detecting phenomena such as deforestation, urbanization, desertification or land artificialization (Foody 2003; Turner *et al.* 2007). Continuous analysis of LULC changes via satellite strengthens monitoring systems for natural disasters such as floods, fires or landslides and thus represents support for early-warning systems (Joyce *et al.* 2009; Leblon *et al.* 2022). This allows urban planners, engineers and decision-makers to better plan land use by identifying sensitive agricultural, urban, forest or flood-prone areas (Lambin *et al.* 2003). LULC can be used as an indicator to determine the evolution of forests and development of urbanization, making it highly valuable in studies of

[1] University of Sciences and Technology of Oran, Laboratory of Analysis and Application of Radiations, Mohamed Boudiaf, Oran 31000, Algeria; e-mail: farid.rahal@univ-usto.dz, ORCID: 0000-0001-7495-8324
[2] University of Sciences and Technology of Oran Laboratory LM2SC, Mohamed Boudiaf, Oran 31000, Algeria; e-mail: fatimazohra.babahamed@univ-usto.dz, ORCID: 0000-0001-7085-2506
*corresponding author

**Received:** 2025-07-15; **Revised:** 2025-11-06; **Accepted:** 2025-11-26

climate change, biodiversity loss, land degradation, greenhouse gas emissions or variation of carbon sinks (Song 2023; Mir *et al.* 2025).

Satellite data related to LULCs can be easily integrated into Geographic Information Systems (GIS) to perform complex spatial analyses, combining seismic, demographic, economic, climatic, hydrological and geological data (Goodchild *et al.* 2021).

Analyzing the interaction between urban growth dynamics and seismic hazard is particularly important. Overlaying maps of urban expansion with those of seismic wave amplification zones is a relevant tool that allows us to assess the vulnerability of the urban fabric to seismic phenomena and also to delineate areas to be avoided in future urbanization projects and to favor development in areas with lower exposure to seismic hazards. For carrying out predictions and scenario studies, there are predictive modeling algorithms that can automatically detect changes in cover between two periods and model future land-use scenarios (Rahman *et al.* 2022; Shivappa *et al.* 2024).

Thus, predictive LULC modeling is a strategic tool for sustainable land management, combining the power of spatial analysis, temporal projection and the integration of heterogeneous data. It is essential for anticipating, planning and adapting land uses in the face of environmental and social challenges.

Modeling methodologies for transitional potential and anticipating potential LULC changes under the influence of geographic variables aim to locate changes that have occurred and are likely to occur in the future. The majority of these models examine LULC transitions using temporal land-use data, which, combined with geographic characteristics, make it possible to predict future LULC situations (Halmy *et al.* 2015).

The Oran province, located in north-western Algeria, is a dynamic and multifaceted region. It is distinguished by its geographical diversity, economic importance, environmental challenges and vulnerabilities. Urban areas in this region have been continuously expanding, which has had a profound impact on the spatial structure of land use (LULC) (Rahal *et al.* 2021). In this work, we modeled the spatio-temporal transition prospects and the future LULC scenario using the MOLUSCE (Modules for Land-Use Change Simulation) plugin in QGIS (Aneesha Satya *et al.* 2020). The MOLUSCE plugin is an open-source model for QGIS 2.0 and later, developed by Asia Air Survey to analyze, model and simulate land use and land cover changes. It integrates several well-known algorithms, such as utility modules, cross-tabulation techniques and algorithmic modules, such as artificial neural networks (ANN), multi-criterionevaluation (MCE), weighting of evidence (WoE), logistic regression (LR) and Monte Carlo cellular automata (CA) models (Muhammad *et al.* 2022).

To simulate spatiotemporal transition possibilities and LULC forecasts for 2030, 2035 and 2040, we used the CA-ANN technique with remote sensing data from 2015 to 2020, with a five-year interval, as well as spatial attributes, a digital elevation model (DEM), slope, and road proximity. After simulating and forecasting LULC, we supplemented it with seismic hazard indicators.

Indeed, areas experiencing urban expansion could be subject to seismic phenomena that can cause enormous destruction, loss of human lives, and socio-economic problems (Parker *et al.* 1995; Alexander 2000; Wenzel *et al.* 2007). The Oran region is also affected by this phenomenon because it is characterized by a complex seismotectonic context and moderate seismic activity associated with the convergence between the African and Eurasian plates (Peláez *et al.* 2006). The region has experienced several destructive earthquakes in history (Baba-Hamed *et al.* 2013), including the 1790 Oran earthquake whose seismic intensity was estimated at level XI on the Modified Mercalli scale. A timely understanding of urban growth in earthquake-prone areas is crucial for seismic risk assessment and urban planning aimed at mitigating the effects of earthquakes (d'Ercole 1995; Guessoum 2012; Dauphiné *et al.* 2013; Durmaz 2017).

The objectives of this study are to analyze the magnitude and evolution of spatiotemporal LULC trends over the last decade through modeling. It also aims to predict future LULC using a model based on artificial neural networks (ANNs). Finally, it aims to cross-reference seismic hazard with current and future artificialized areas in the Oran region.

# Methods

## The study area

Located on the north-west coast of Algeria, the wilaya of Oran, shown in Fig. 1, is one of the most dynamic in the country. It is distinguished by its economic importance, cultural richness and strategic role in the Mediterranean.

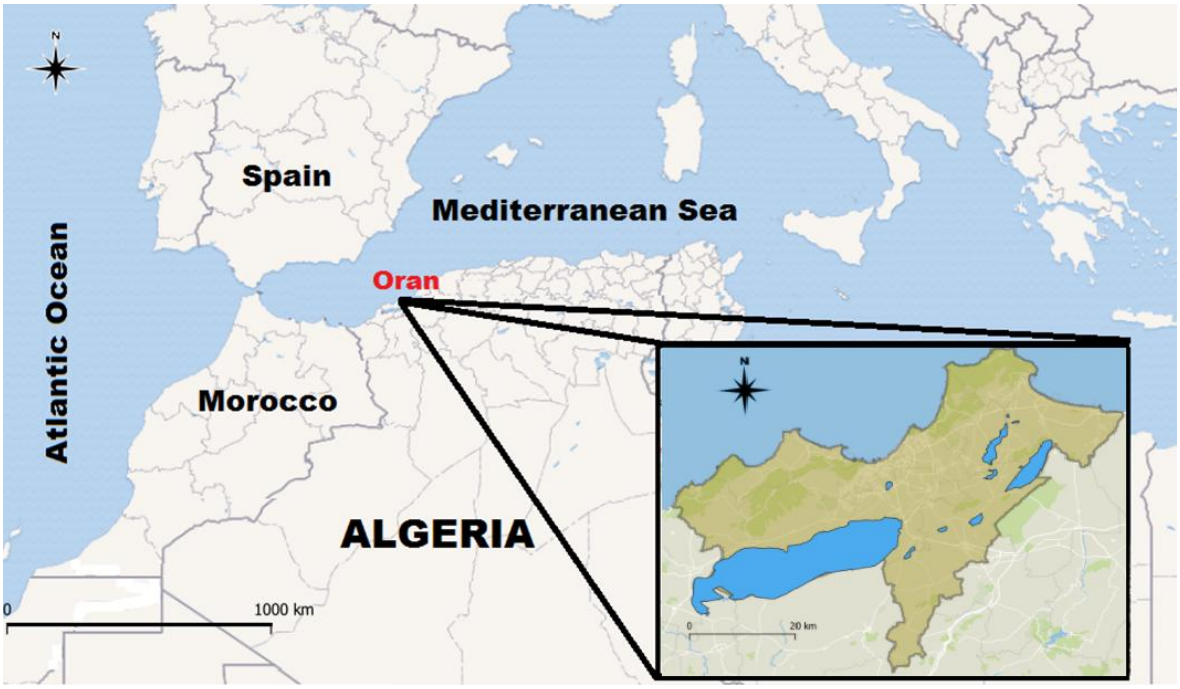


Fig.1. Study area and its location relative to Algeria and the western Mediterranean Sea

The second largest city in the country after Algiers, Oran is also a major university, industrial and port center (Rahal *et al.* 2018).

Oran has a semi-arid Mediterranean climate, with average annual precipitation ranging between 300 and 400 mm. The terrain is characterized by a maritime facade composed of rocky coasts stretching from the Arzew Mountains to Mers el-Kébir in the west, and from Cape Lindles to Cape Sigal in the east. The M'leta Plain and the Oran-Gdyel Plateau are also notable geographical features of the region (Bellal *et al.* 2015).

The Oran region is characterized by several distinct types of geological formations (Benabdellah 2011):

- Miocene formations are found in the area between the base of Mount Murdjajo and Misserghin. These are limestones and calcareous marls, with, in the lower part of the series, beds of fine sandstone associated with beds of yellow marl and some beds of lumachelle. Toward the south, the facies changes, with marl and clay deposits becoming increasingly prominent.
- Quaternary deposits are located in the Es-Sénia, Chteibo and Daia Morsli regions. They are characterized by layers of tufa limestone, highly gypsiferous and salt-bearing, fissured, with numerous lenses of detrital clay, silt and loess, and the presence of lignite. Recent field investigations have identified two major active structures (Yelles-Chaouche *et al.* 2006) that can generate significant earthquakes:

- The North Sebkha Fault, which extends ~15 km in a NE–SW direction. It delimits the Murdjadjo Mountains to the north and the Great Sebkha Plain to the south (the Mleta Basin);
- The South Sebkha Fault, which extends ~30 km along the Tessala Mountains, oriented NE–SW. It intersects the foothills of the lower Pleistocene to Holocene alluvial layers, separating the Great Sebkha of Oran (Mleta Basin) to the north from the Tessala Mountains to the south.

Since Algeria's independence in 1962, Oran has experienced rapid urbanization, marked by the emergence of new urban centers, both legal and informal. This expansion has led to a fragmentation of the urban space, with notable disparities between neighborhoods in terms of infrastructure and services. Studies have highlighted the extent of this fragmentation and the challenges it poses for urban planning (Bendjelid 1998).

The metropolitanization of Oran is accompanied by the emergence of new commercial centers on the outskirts. These spaces, often driven by private actors, are becoming hubs of consumption and distribution, competing with the traditional city center. This phenomenon illustrates

the transformation of commercial practices and the redistribution of economic activities in the city (Otmane *et al.* 2023).

Informal housing constitutes a significant portion of Oran's urban landscape. Neighborhoods such as Les Planteurs have seen their populations grow rapidly, particularly due to internal migration flows linked to economic and security factors. These dynamics have often led to unplanned urbanization, posing challenges for social integration and access to basic services (Lakjaa 2008).

Unplanned urbanization most often occurs in high-risk areas such as floodplains, landslide-prone areas, and areas with increased seismic hazards.

## Data collection

Satellite images for 2015 and 2020 were obtained from the Landsat 8 OLI satellite, while those for 2025 were obtained from the Landsat 9 OLI-2 satellite, which were processed and interpreted. Landsat satellite data are freely available from the US Geological Survey EarthExplorer website (USGS 2025).

The images used in this study are dated 07/11/2015, 29/06/2020 and 11/02/2025, respectively. These images were selected for their high quality, particularly due to the absence of cloud cover. However, seasonal variations may affect the accurate classification of surfaces. For this reason, an in-depth photo-interpretation was carried out, based on a thorough knowledge of the study area.

Radiometric calibration was performed to convert pixel digital numbers (DN) into physical units such as radiance and reflectance.

Four main land cover classes are included in the data, namely artificial land, vegetation, water, and bare soil, with a spatial resolution of 30 m. Photo-interpretations and kappa coefficient tests are used to ensure the accuracy of LULC categorization. The digital elevation model (DEM) was also acquired from the United States Geological Survey (USGS). This is Shuttle Radar Topography Mission (SRTM) satellite data that was collected during an 11-day mission in February 2000 and is available for free download for about 80% of the globe. (Athmania *et al.* 2014). Slopes were estimated using the DEM, while proximity factors, such as distance to roads, were estimated by the Euclidean distance method in QGIS 3.40. The study area was delineated and projected to WGS 1984 UTM zone 30N after data collection. After extracting and projecting the study area, we used resampling techniques in QGIS to correct for differences in spatial resolution between the collected data.

## LULC Classification

Part of the analysis of the urban evolution of the city of Oran between 2015 and 2025 and the identification of the different built-up areas involved use of the Semi-automatic Classification Plugin (SCP), integrated into QGIS software. This enabled the determination of the four main land-use classes: artificial land, vegetation, water, and bare soil. Lakes and large bodies of water were excluded from the classification. Only small- and medium-scale hydrological features are classified as water.

Natural barriers such as Mount Murdjadjo to the west and the sebkha (temporary salt lake) to the south have caused the expansion of the city of Oran to be eastward, driven by demographic pressure, urban planning choices, and land availability. Indeed, since the 1980s, Oran has experienced significant population growth, fueled by rural exodus and industrialization. This population increase has led to increased demand for housing and infrastructure, pushing urbanization to peripheral areas, particularly to the east of the city (Kadri *et al.* 2015), which offer relatively flat and available land, facilitating construction projects. However, this expansion has often come at the expense of peri-urban agricultural land, thus threatening local agriculture and leading to significant landscape changes. Land pressure has led to a decrease in the area of agricultural land, affecting local food production and biodiversity (Maachou *et al.* 2016). Authorities have implemented planning instruments, such as the “Master Plan for Urban Development” (PDAU), to regulate urban development. However, the implementation of these plans has often been ineffective, leading to uncontrolled urbanization. Thus, urban planning documents, although necessary, have failed to effectively control urban expansion, particularly due to their lack of flexibility and adaptation to local realities. Furthermore, Oran's urban growth has led to peri-urbanization, with expansion into peripheral municipalities such as Gdyel and Arzew. For example, between 2008 and 2018, Arzew recorded a 29.3% population increase, reflecting a general urbanization trend in the region (Kacemi 2009; Bounoua *et al.* 2023). This dynamic is fueled by increased real-estate production and a deconcentration of the population from urban centers to the peripheries (Trache *et al.* 2020). LULC classifications

can thus contribute to a better understanding of the development of urbanization within the wilaya of Oran.

## Analysis and prediction of changes and modeling of transition potential

LULC predictive modeling involves using mathematical, statistical or artificial-intelligence-based tools to forecast future changes in space and time. It aims to anticipate the spatial dynamics of land-use change and simulate different development scenarios such as urban growth or resource conservation policies. It also aims to assess the environmental, social and economic impacts of land-use changes. Furthermore, it can support public decision-making through data-driven planning. It allows for the testing of different scenarios such as urban densification or urban sprawl (Verburg *et al.* 2004; Pontius *et al.* 2008; Li *et al.* 2021). Finally, it allows for the assessment of different types of risks associated with territorial development.

Predictive approaches are often based on tools such as GIS, remote sensing, statistical models, cellular automata, neural networks and machine learning. They integrate numerous spatial and temporal data sources, providing a comprehensive and coherent view (Eastman 2006; Al-Dousari *et al.* 2023).

The introduction of artificial intelligence through tools such as neural networks and machine learning algorithms improves the accuracy and robustness of predictions, as well as the ability to capture complex dynamics (Aburas *et al.* 2016; Yang *et al.* 2020). The main categories of models used in predictive land use and land cover approaches are presented in Table 1.

Table 1

The main types of models used in predictive approaches concerning LULC

| Model | Description | Reference |
|---|---|---|
| CA-Markov | Combines Markov chains (transition probabilities) and cellular automata (spatial dynamics) | Floreano *et al.* 2021 |
| ANN (Neural networks) | Predicts changes from past examples by learning the complex relationships between variables | Aburas *et al.* 2016 |
| SLEUTH | Specific urban growth model based on transition rules | Clarke *et al.* 1997 |
| Random Forest, SVM, … | Supervised learning widely used in LULC classification with satellite images | Rodriguez-Galiano *et al.* 2012 |

We used the QGIS MOLUSCE (Modules for Land-Use Change Simulation) plugin to estimate spatiotemporal changes and calculate land-use transitions between the research intervals (2015, 2020 and 2025). To model transition potential, we used the multi-layer perceptron (ANN) approach. DEM, slope, and distance to roads were used as explanatory factors. These variables are often used in land-use change analysis because they provide reproducible data on physical and anthropogenic influences on land-use dynamics. The simulated models reduce the dynamics of composite urban structures and make them more understandable. The CA-ANN technique was used with the MOLUSCE plugin to model transition potentials and simulate the future. This plugin efficiently performs land-use change analyses and is particularly suited for assessing spatio-temporal land-use changes, predicting transition prospects and simulating future scenarios (Muhammad *et al.* 2022).

Using LULC data from 2000 and 2010, explanatory variables and transition matrices, we projected LULC for 2020. To validate the accuracy of the model and forecasts, the MOLUSCE plugin offers a kappa validation technique and a comparison of actual and projected LULC images. In the ANN training process, 100 iterations and a neighborhood value of 3 pixels, a learning rate of 0.001, 12 hidden layers, and a momentum of 0.05 were chosen to project the LULC for 2020. After obtaining satisfactory results during model validation, we used the LULC data from 2010 and 2020 to predict the LULC in 2030, and those from

2000 and 2020 for 2040. The predicted data for 2030 and 2040 were used to predict the LULC for 2050 (Fig. 2).

To obtain the annual rate of change for each land-use type, the difference between the last year and the first year, which represents the magnitude of change between the corresponding years, was divided by the year and the initial period. Based on the work of Puyravaud (2003), we used (eq.1) to assess the spatio-temporal magnitude and rate of change of land-use categories:

$$\mathrm{ARC} = \left(\left(\frac{F_y}{I_y}\right)^{\frac{1}{t}} - 1\right) \cdot 100 \qquad (1)$$

where:
ARC – the annual rate of change in LULC categories [%];
Iy and Fy – the initial and final year areas, respectively;
t – the time interval.

## Seismic Hazard Level Assessment

The seismic hazard assessment criterion primarily relies on the regional hazard level while explicitly accounting for site effects related to both topography and soil lithology. Topographic site effects occur when local surface conditions, such as slopes or irregular relief, significantly alter the amplitude and spatial distribution of seismic ground motions. Similarly, the presence of soft soil layers overlying a rigid seismic bedrock can lead to an amplification of ground motion during an earthquake, a phenomenon referred to as the "lithological site effect".

In the Algerian seismic code (RPA 99 – 2003 version), these effects are incorporated through a soil classification system associated with specific amplification coefficients. The soil classes, as presented for example in Table 2 of the code, are defined based on the Vs30 parameter, which represents the average shear-wave velocity within the upper 30 m of the soil profile.

Table 2

Classification of soils according to the Vs parameter (Baba-Hamed *et al.* 2024)

| Category | Description | Vs ($m \cdot s^{-1}$) (average shear wave velocity) |
|---|---|---|
| S1 | Rock | 800 |
| S2 | Stiff soil | $400 < Vs \leq 800$ |
| S3 | Soft soil | $200 < Vs \leq 400$ |
| S4 | Very soft soil | $100 < Vs \leq 200$ |

Table 3

Consideration of site effects scoring (Borfecchia *et al.* 2016)

| | | |
|---|---|---|
| Topographic amplification score | Classification of slopes | St |
| | Plane surface, slope or isolated relief with a slope angle (p) less than 15° | 1 |
| | Slope with ($15° \leq p < 30°$) | 1.2 |
| | Steep to very steep slope with ($p \geq 30°$) | 1.4 |
| | | |
| Stratigraphic amplification score | Classification of soils | Ss |
| | S1: Rock | 1 |
| | S2: Stiff soil | 1.1 |
| | S3: Soft soil | 1.15 |
| | S4: Very soft soil | 1.25 |

The local hazard level in terms of PGA (peak ground accelerations) (eq.2) is calculated at all points of the studied area, by applying the topographic and lithological amplification coefficients shown in Table 3.

$$PGA = ag \cdot Ss \cdot St \quad (2)$$

where:
ag – the reference ground acceleration;
Ss and St – the soil and the topographic factor.

# Results and discussion

## Analysis of spatiotemporal changes

The changes in LULC classifications from 2015 to 2025, shown in Table 4 and Figure 2, indicate an increase in artificialized areas at the expense of vegetation. The areas occupied by bodies of water have increased slightly, as has the bare soil class.

Table 4

Evolution of LULC classes from 2015 to 2025

| | 2015 | | 2020 | | 2025 | | ARC [%] |
|---|---|---|---|---|---|---|---|
| LULC Type | Area [km²] | % | Area [km²] | % | Area [km²] | % | |
| Water | 3,552.30 | 0.20 | 4,939.20 | 0.28 | 5,384.70 | 0.31 | 4.25 |
| Built-up area | 168,949.80 | 9.59 | 175,552.30 | 9.97 | 243,486.90 | 13.83 | 3.72 |
| Vegetation | 381,216.60 | 21.65 | 355,584.60 | 20.19 | 291,735.90 | 16.56 | -2.64 |
| Bare soil | 1,207,484.10 | 68.56 | 1,225,126.70 | 69.56 | 1,220,595.30 | 69.30 | 0.11 |

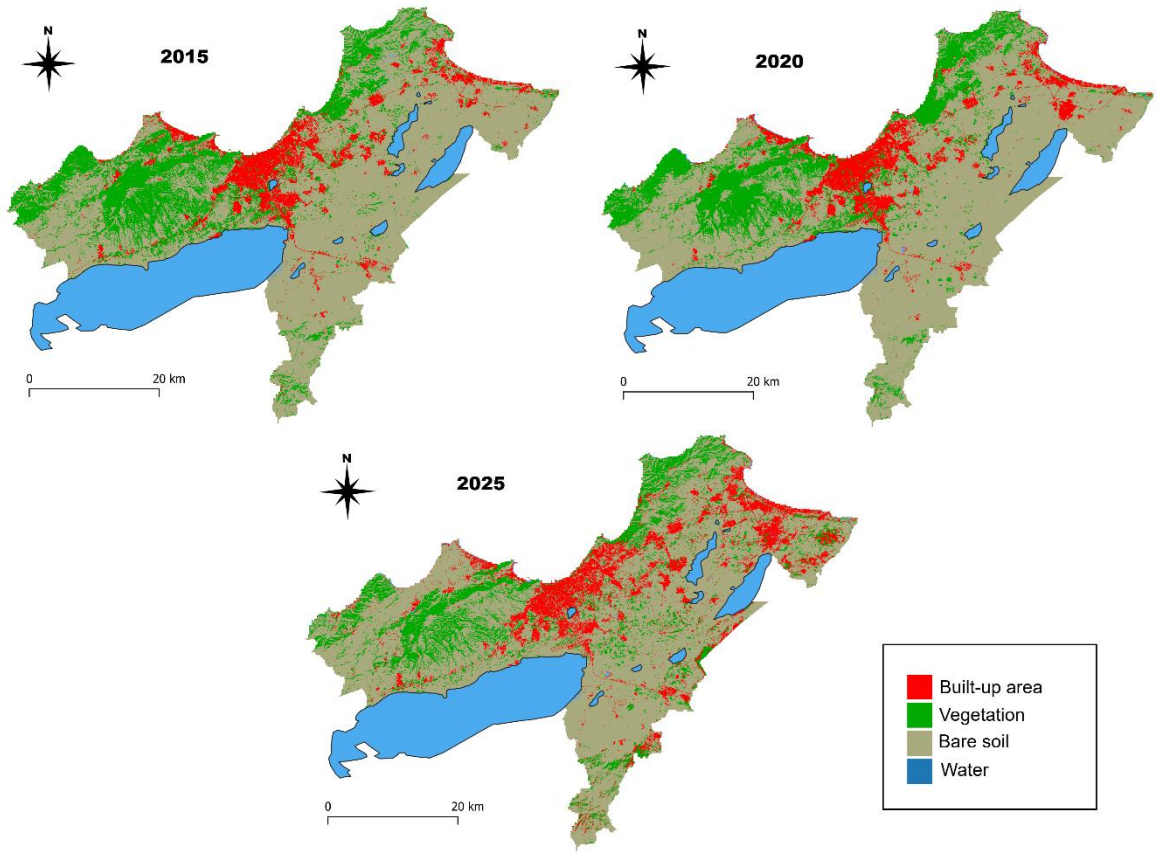


Fig. 2. LULC classification of the Wilaya of Oran from 2015 to 2025

## Prediction of Artificial Surface Changes

The prediction of artificial surface changes seeks to estimate the temporal dynamics of both the extent and the spatial distribution of built-up, industrial and other anthropogenically transformed areas.

The main factors influencing the evolution of artificial surfaces are slope, proximity to roads and DTM (Muhammad *et al.* 2022). These factors are illustrated in Figure 3.

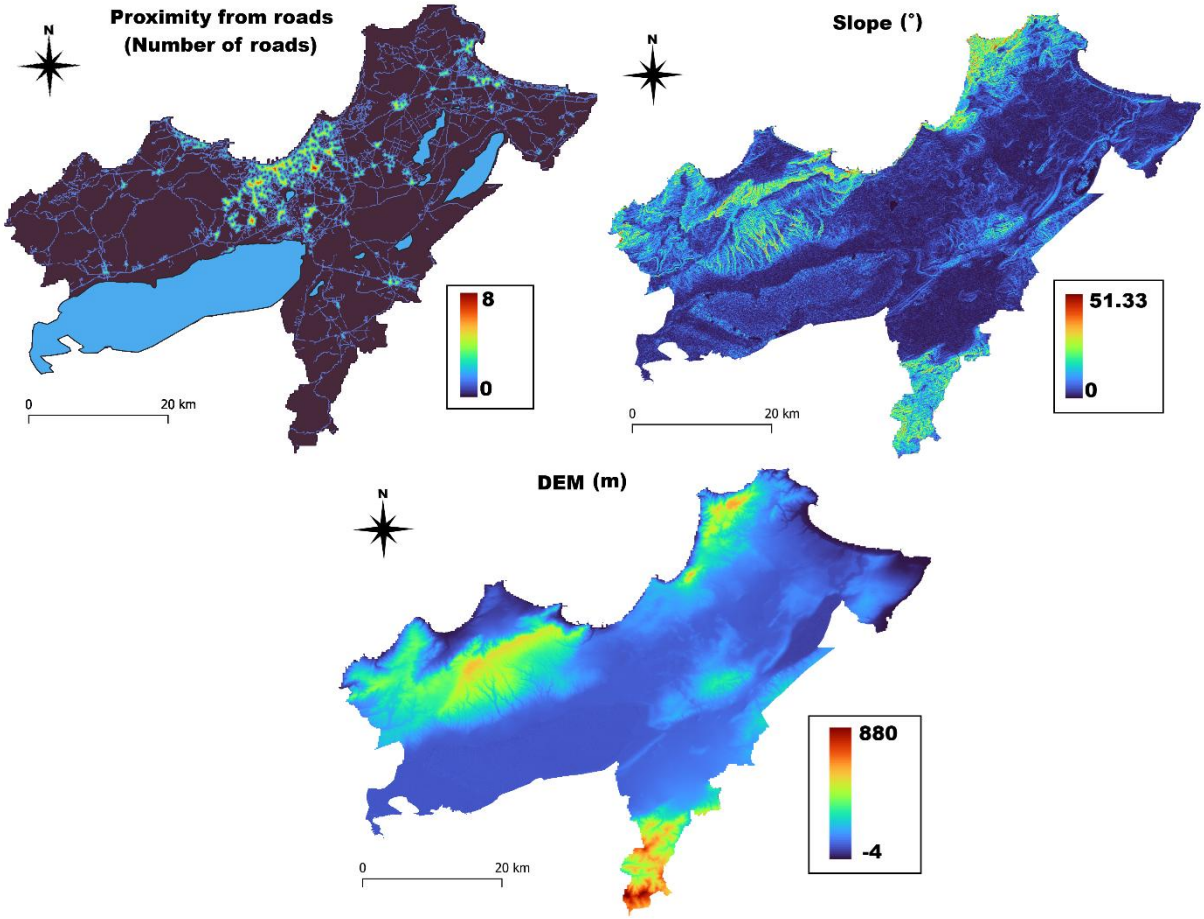


Fig. 3. Spatial variables used in predicting the evolution of artificial surfaces for the wilaya of Oran

The modeling and prediction of the transition potential were performed using the CA-ANN approach using the MOLUSCE plugin.

In the MOLUSCE framework, land-use change dynamics are simulated through four complementary steps:

- Estimation of global transitions (Markov chain)

The global probability of transition from class i to class j is given by the Markov transition matrix (Pontius *et al.* 2005; Eastman *et al.* 2020).

$$M_{i,j} = \frac{\text{number of cells changing from i to j}}{\text{total number of cells initially in i}} \quad (3)$$

- Evaluation of local transition potential

In this work, the transition potential of a cell to another class is computed from explanatory variables using a multilayer perceptron:

$$h^{l} = \tanh\left(h^{(l-1)} \cdot W^{(l)} \cdot b^{(l)}\right) \quad (4)$$

where:

$h^{(0)}=x$ denotes the input vector containing the explanatory variables (e.g., slope, proximity to roads, or previous land-use class);

l – indexes the hidden layers of the network;

$h^{(l)}$ – the activation vector of layer l (i.e., the non-linear transformation of the weighted sum of the previous layer's outputs);

$W^{(l)}$ – the weight matrix connecting layer l−1 to layer l (its coefficients quantify the contribution of each input to each neuron);
$b^{(l)}$ – the bias vector added to each neuron to shift the activation and increase model flexibility;
tanh(·) – the nonlinear activation function applied element-wise to produce bounded outputs and allow the network to model complex relationships.
- Integration of neighborhood effects (cellular automaton)
Spatial influence is represented by a neighborhood factor:

$$N_{i,c} = \frac{\text{number of neighbouring cells of i belonging to c}}{\text{total number of neighbouring cells considered}} \quad (5)$$

where:
i – the focal cell for which the transition probability is being evaluated;
c – indexes the land-use/land-cover class under consideration
- Final change probability
These components are combined to estimate the probability that a cell i will change to class c at time t+1:

$$P_{i\to c}(t+1) = M_{i\to c} \cdot \hat{y}_{i,c} \cdot N_{i,c} \quad (6)$$

where:
$M_{i\to c}$ – the global Markov probability;
$\hat{y}_{i,c}$ – the transition potential (ANN);
$N_{i,c}$ – the neighborhood factor.

LULC data from 2015 to 2020, along with the spatial variables presented in Figure 3, were used to project LULC for 2025.

Model validation in MOLUSCE is conducted by comparing the simulated land-use map with an observed map at the target date using standard agreement measures like overall accuracy and Cohen's kappa statistics. This process quantifies both the quantity and location accuracy of the predicted land-use transitions

The validation factor obtained a kappa of 0.79. After obtaining the projected LULC, a comparison of the actual 2025 LULC with the projected data was performed. This comparison yielded an overall accuracy of 82.59% and an overall kappa of 0.69. Figure 4 presents the actual and projected maps for 2025 with regard to artificialized surfaces.

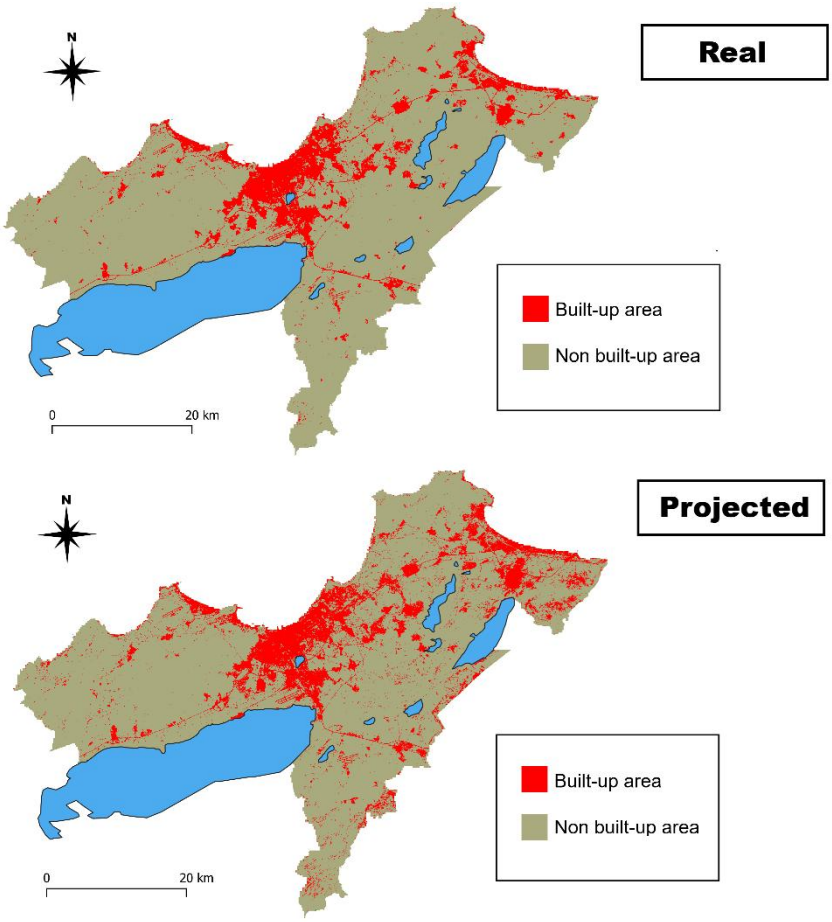


Fig. 4. Spatial comparison between the observed extent of artificialized surfaces in 2025 and the areas projected by the model for the same year within Oran Province

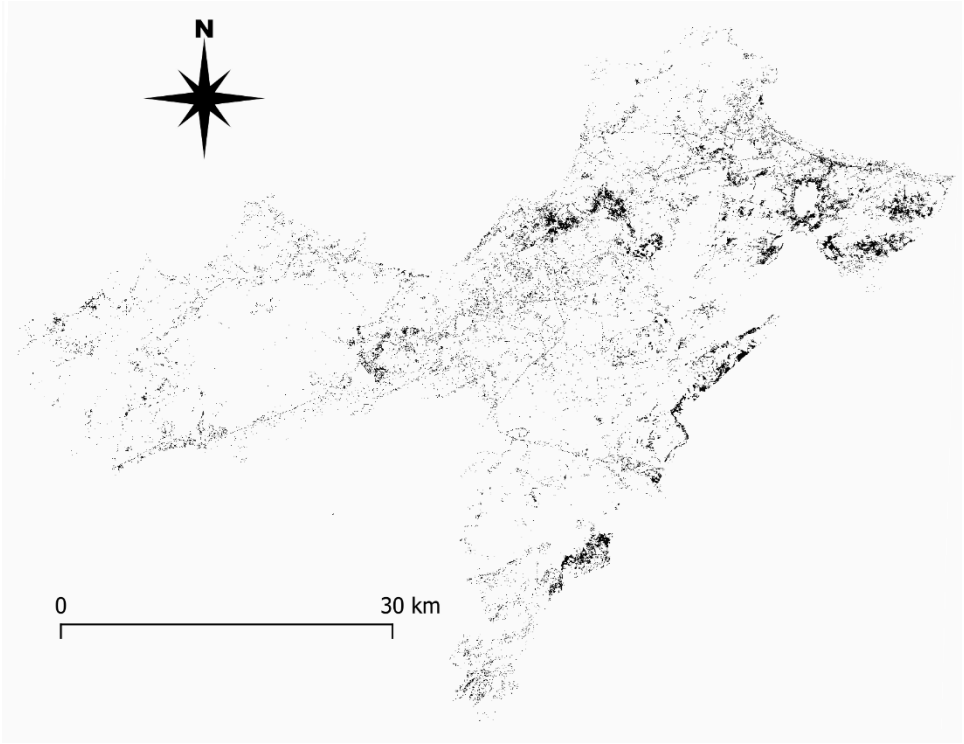


Fig. 5. The pixels that have changed between the map of actual artificialized surfaces in 2025 and those projected for the province of Oran

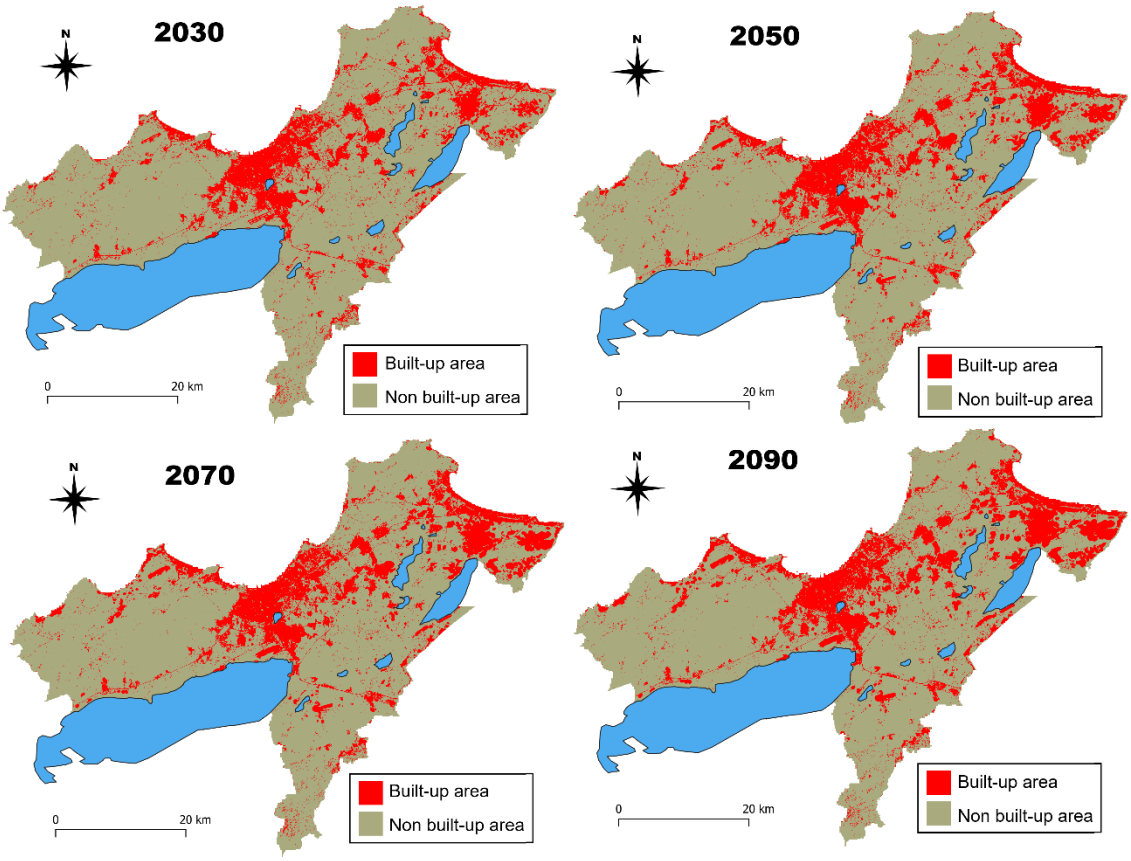


Fig. 6. Projected spatial extent of built-upareas within Oran Province for the years 2030, 2050, 2070, and 2090, as derived from the applied predictive modelling approach

The differences between the two maps, particularly in the south and east of the wilaya, are explained by the creation of a vast industrial zone of 596 hectares dedicated to the automobile industry in the locality of Tafraoui in 2022, the extension of the steel and petrochemical industries in the locality of Arzew, as well as by the various developments linked to the creation of these economic activity zones. These differences are shown in Figure 5.

After obtaining reasonable results during model validation, predictions of the evolution of built-up areas were made for 2030 to 2090 with a time step of five years. Figure 6 shows built-up areas for 2030, 2050, 2070 and 2090.

It is predicted that built-up areas for the years 2030, 2050, 2070 and 2090 will represent 18.34%, 20.06%, 21.44% and 22.62% of the surface area of the province of Oran, respectively. Because future socio-economic and environmental conditions are uncertain, the projections are treated as scenario-based simulations rather than deterministic forecasts, providing plausible spatial patterns.

## Assessment of seismic hazard levels

The amplification of the topographic site effect was considered through the variation of slopes in the study area based on the SRTM (Shuttle Radar Topography Mission) digital elevation model, as shown in Figure 7a. While the lithological site effect, shown in Figure 7b, was assessed using Vs30 (the time-averaged shear-wave velocity to 30 m depth) estimates from the USGS (United States Geological Survey) Global Vs30 Map service, which derives Vs30 from topographic slopes (Wald *et al.* 2007).

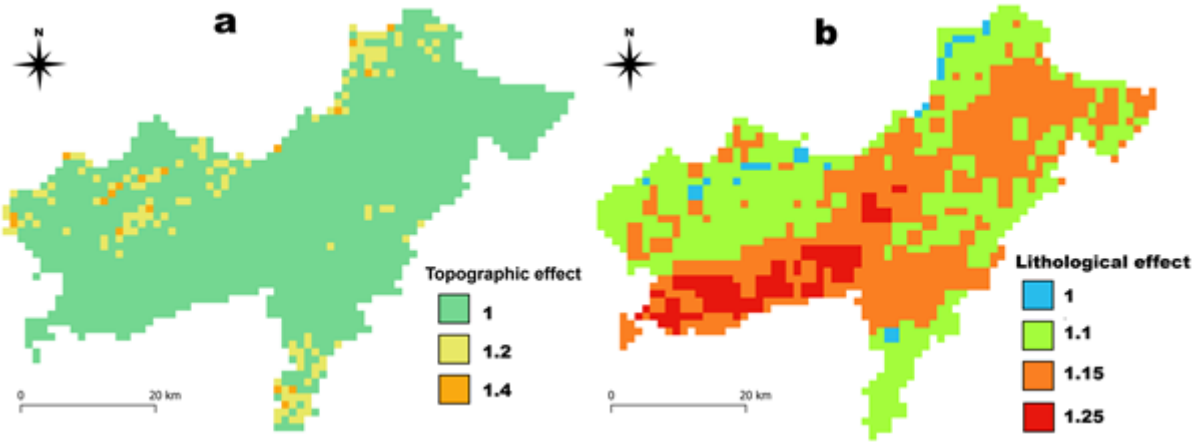


Fig. 7. Topographical site effects and lithological site effects of the province of Oran

The regional seismic hazard in the Oran province was previously studied by Peláez *et al.* (2006) and presented in terms of average horizontal acceleration ($m \cdot s^{-2}$) on rocky ground in the form of zoning maps for 100-year return periods. The unit for Peak Ground Acceleration (PGA) is typically expressed as a fraction or multiple of g, the standard acceleration due to gravity (approximately 9.8 $m \cdot s^{-2}$)

The probable values of PGA in the average case are 0.068 g for a 100-year return period and 0.138 g for a 475-year return period.

The PGA in the worst-case scenario is 0.095 g for a 100-year return period and 0.18 g for a 475-year return period. We calculated the predicted local seismic hazard for several scenarios in the Wilaya of Oran, at all locations within the study area, by superimposing the lithological and topographical impacts of the site. Figure 8 presents the hazard levels of the various artificialized surfaces predicted for 2050 over a 100-year return period, expressed in terms of a PGA of 0.095 g.

The seismic hazard levels are distributed according to the following classification.

H1: Very Low when PGA is less than 0.07g;
H2: Low if $0.07 \leq PGA < 0.11$ g;
H3: Moderate if $0.11\ g \leq PGA < 0.16$ g;
H4: High if $0.16\ g \leq PGA < 0.3$ g;
H5: Very High if PGA ≥0.3g.

The hazard level of the various maps of built--upareas predicted for the years 2030, 2050, 2070 and 2090 is examined.

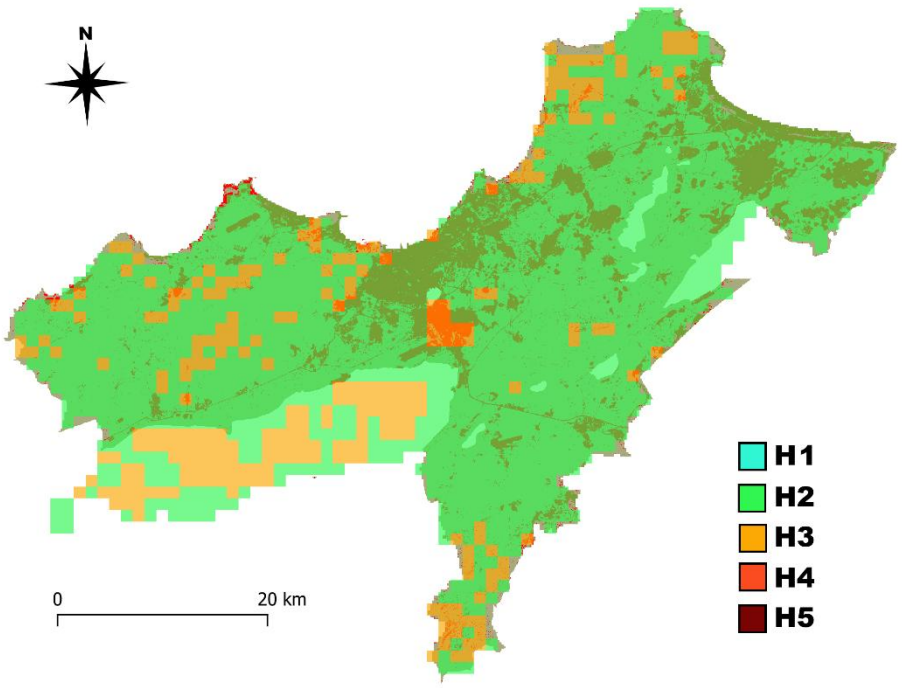


Fig. 8. Hazard levels for built-up areas predicted for 2050 over a 100-year return period, for a peak ground acceleration (PGA) of 0.095 g

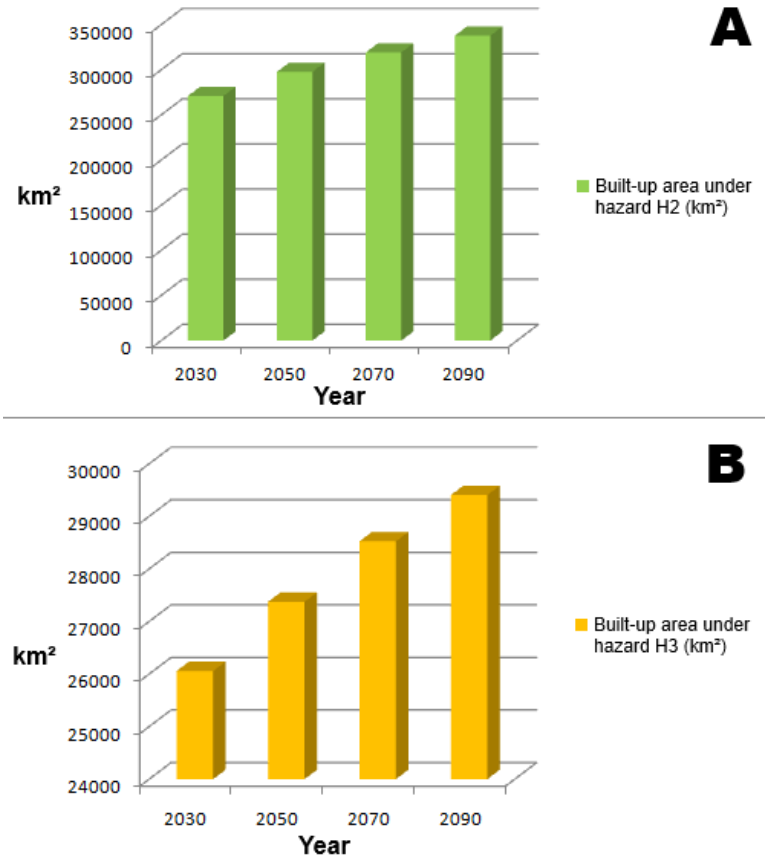


Fig. 9. A. Changes in built-up areas affected by the H2 hazard according to predictions made for 2030–90
B. Changes in artificial areas affected by the H3 hazard according to predictions made for 2030–90

Figure 9 shows the surface areas of built-up areas during the period 2030–90, corresponding to the different hazard levels for a 100-year return period. The areas affected by hazard H2 are significantly larger than the areas affected by hazard H3. This explains the large difference between the changes in built-up areas affected by these two hazards.

The predictions show that there will be a significant increase in the level of urbanization in areas representing an average H3 seismic hazard in the coming years and could reach 26,058 km², 27,373 km², 28,524 km² and 29,403 km², respectively, by 2030, 2050, 2070 and 2090.

It is therefore important to anticipate this risky situation by prioritizing urbanization in areas where the seismic hazard is low.

## Conclusion

This study demonstrates that analyzing the spatiotemporal dynamics of land-use/land-cover (LULC) change and simulating future scenarios can provide a forward-looking assessment of hazards affecting newly urbanized areas. Among these, seismic hazard remains a critical concern for the urban zones of Oran Province, which hosts major active fault structures capable of generating significant earthquakes. By classifying artificial surfaces from a Landsat time series and projecting their evolution for 2030–90 using an artificial neural network model, we quantified and mapped the spatial and temporal trajectories of urban expansion. The projections reveal substantial future urban growth within areas of moderate seismic hazard, underscoring the need for proactive territorial planning policies that prioritize development in low-hazard zones to reduce exposure to seismic risk.

However, it should be noted that the socio-economic and environmental conditions of the study area may evolve in a non-stationary manner over the long term. Future work could extend this study by integrating higher-resolution remote-sensing data and dynamic socio-economic and environmental covariates to better represent the non-stationarity of the drivers of land-use change.

The authors would like to thank the US Geological Survey EarthExplorer, for providing the satellite images used in this work.

## References

Aburas M. M., Ho Y. M., Ramli M. F., Ash'aari Z.H. 2016. The simulation and prediction of spatio-temporal urban growth trends using cellular automata models: A review. *International Journal of Applied Earth Observation and Geoinformation* 52: 380--389. DOI: 10.1016/j.jag.2016.07.007

Al-Dousari A.E., Mishra A., Singh S. 2023. Land use land cover change detection and urban sprawl prediction for Kuwait metropolitan region, using multi-layer perceptron neural networks (MLPNN). *The Egyptian Journal of Remote Sensing and Space Science* 26(2): 381-392. DOI: 10.1016/j.ejrs.2023.05.003

Alexander D. 2000. Confronting Catastrophe: New Perspectives on Natural Disasters. Oxford, Oxford University Press.

Aneesha Satya B., Shashi M., Deva P. 2020. Future land use land cover scenario simulation using open source GIS for the city of Warangal, Telangana, India. *Applied Geomatics* 12(3): 281-290. DOI:10.1007/s12518-020-00298-4

Athmania D., Achour H. 2014. External validation of the ASTER GDEM2, GMTED2010 and CGIAR-CSI-SRTM v4.1 free access digital elevation models (DEMs) in Tunisia and Algeria. *Remote Sensing* 6(5): 4600-4620. DOI: 10.3390/rs6054600

Baba-Hamed F.Z., Rahal D.D., Rahal F. 2013. Seismic risk assessment of Algerian buildings in urban area. *Journal of Civil Engineering and Management* 19(3): 348--363. DOI: 10.3846/13923730.2012.744772

Baba-Hamed F.Z., Rahal F., Guenanou F. 2024. Seismic vulnerability assessment of bridges. The case of the Oran region, Algeria. *Revista Facultad de Ingeniería Universidad de Antioquia* 110 : 23-30. DOI: 10.17533/udea.redin.20221209

Bellal S.A., Mokrane S., Ghodbani T., Dari O. 2015. Ressources, usagers et gestionnaires de l'eau en zone semi-aride: Le cas de la wilaya d'Oran (ouest algérien). *Territoire en mouvement Revue de géographie et aménagement. Territory in movement Journal of geography and planning* 25-26. DOI: 10.4000/tem.2859

Bendjelid A. 1998. La fragmentation de l'espace urbain d'Oran (Algérie). Mécanismes, acteurs et aménagement urbain. *Insaniyat* 2(2): 61--84. DOI: 10.4000/insaniyat.11804

Borfecchia F., De Canio G., De Cecco L., Giocoli A., Grauso S., La Porta L., Zini A. 2016. Mapping the earthquake-induced landslide hazard around the main oil pipeline network of the Agri Valley (Basilicata, southern Italy) by means of two GIS-based modelling approaches. *Natural Hazards* 81(2) : 759- - 777. DOI: 10.1007/s11069-015-2104-0

Bounoua L., Bachir N., Souidi H., Bahi H., Lagmiri S., Khebiza M.Y., Thome K. 2023. Sustainable development in Algeria's urban areas: population growth and land consumption. *Urban Science* 7(1) : 29. DOI: 10.3390/urbansci7010029

Charnell R.L., Maul G.A. 1973. Oceanic observation of New York bight by Erts-1. *Nature* 242(5398) : 451-452. DOI: 10.1038/242451a0

Clarke K.C., Hoppen S., Gaydos L. 1997. A self-modifying cellular automaton model of historical urbanization in the San Francisco Bay area. *Environment and planning B: Planning and design* 24(2): 247-261. DOI: 10.1068/b240247

Cohen W.B., Goward S.N. 2004. Landsat's role in ecological applications of remote sensing. *Bioscience* 54(6): 535-545.DOI: 10.1641/0006-3568(2004)054[0535:LRIEAO]2.0.CO;2

Dauphiné A., Provitolo D. 2013. Risques et catastrophes: observer, spatialiser, comprendre, gérer. Armand Colin. DOI: 10.3917/arco.dauph.2013.01

Drusch M., Del Bello U., Carlier S., Colin O., Fernandez V., Gascon F., Bargellini P. 2012. Sentinel-2: ESA's optical high-resolution mission for GMES operational services. *Remote sensing of Environment* 120: 25-36. DOI: 10.1016/j.rse.2011.11.026

Durmaz N. 2017. Prévention des risques par la maîtrise de l'urbanisation. Le cas d'Istanbul. *Revue des sciences sociales* 57: 64-75. DOI: 10.4000/revss.369

d'Ercole R., Thouret J.C., Aste J.P., Dollfus O., Gupta A. 1995. Croissance urbaine et risques naturels: présentation introductive. *Bulletin de l'Association de géographes français* 4: 311-338.

Eastman J.R. 2006. IDRISI Andes tutorial. Clark Labs., Clark University, Worcester, MA.

Eastman J.R., He J. 2020. A regression-based procedure for Markov transition probability estimation in land change modeling. *Land* 9(11): 407. DOI: 10.3390/land9110407

Foody G.M. 2003. Remote sensing of tropical forest environments: towards the monitoring of environmental resources for sustainable development. *International journal of remote sensing* 24(20): 4035-4046. DOI: 10.1080/0143116031000103853

Floreano I.X., de Moraes L.A.F. 2021. Land use/land cover (LULC) analysis (2009–2019) with Google Earth Engine and 2030 prediction using Markov-CA in the Rondônia State, Brazil. *Environmental Monitoring and Assessment* 193(4): 239. DOI: 10.1007/s10661-021-09016-y

Goodchild M.F., Longley P.A. 2021. Geographic information science. [In:] Handbook of Regional Science. Berlin, Heidelberg: Springer Berlin Heidelberg : 1597-1614. DOI: 10.1007/978-3-662-60723-7_61

Guessoum N. 2012. Apport des études de microzonage sismique dans l'aménagement de futures nouvelles villes : cas de la nouvelle ville de Sidi Abdellah (Algérie). *Knowing to manage the territory, protect the environment, and evaluate the cultural heritage*. Rome, Italy, 6–10 May 2012.

Halmy M.W.A., Gessler P.E., Hicke J.A., Salem B.B. 2015. Land use/land cover change detection and prediction in the north-western coastal desert of Egypt using Markov-CA. *Applied geography* 63: 101-112. DOI: 10.1016/j.apgeog.2015.06.015

Joyce K.E., Belliss S.E., Samsonov S.V., McNeill S.J., Glassey P.J. 2009. A review of the status of satellite remote sensing and image processing techniques for mapping natural hazards and disasters. *Progress in physical geography* 33(2): 183-207. DOI: 10.1177/0309133309339563

Kacemi M. 2009. Protection du littoral en Algérie entre gestion et législation. Le cas du pôle industriel d'Arzew (Oran, Algérie). *Droit et société* 3 : 687-701. DOI: 10.3917/drs.073.0687

Kadri Y., Madani M. 2015. L'agglomération oranaise (Algérie) entre instruments d'urbanisme et processus d'urbanisation. *EchoGéo* 34. DOI: 10.4000/echogeo.14386

Lakjaa A. 2008. Oran, une ville algérienne reconquise; Un centre historique en mutation. *L'année du Maghreb*, (IV), 441-456. DOI: 10.4000/anneemaghreb.472

Lambin E.F., Geist H.J., Lepers E. 2003. Dynamics of land-use and land-cover change in tropical regions. *Annual review of environment and resources* 28(1): 205-241. DOI:10.1146/annurev.energy.28.050302.105459

Leblon B., Ogunjobi Oluwamuyiwa F., Lingua E., LaRocque A. 2022. Fire severity assessment of an alpine forest fire with Sentinel-2 imagery. *The International Archives of the Photogrammetry, Remote Sensing and Spatial Information Sciences* 43: 1115-1120. DOI:10.5194/isprs-archives-XLIII-B3-2022-1115-2022

Li X., Zhang J., Li Z., Hu T., Wu Q., Yang J., Wang X. 2021. Critical role of temporal contexts in evaluating urban cellular automata models. *GIScience & Remote Sensing* 58(6): 799-811. DOI: 10.1080/15481603.2021.1946261

Lu D., Weng Q. 2007. A survey of image classification methods and techniques for improving classification performance. *International Journal of Remote Sensing* 28(5): 823-870. DOI: 10.1080/01431160600746456

Maachou H.M., Otmane T. 2016. L'agriculture périurbaine à Oran (Algérie): diversification et stratégies d'adaptation. *Cahiers Agricultures* 25(2): 25002. DOI: 10.1051/cagri/2016011

Mir Y.H., Mir S., Ganie M.A., Bhat J.A., Shah A.M., Mushtaq M., Irshad I. 2025. Overview of Land Use and Land Cover Change and Its Impacts on Natural Resources. [In:] *Ecologically Mediated Development: Promoting Biodiversity Conservation and Food Security*. Singapore, Springer Nature Singapore: 101-130. DOI: 10.1007/978-981-96-2413-3_5

Muhammad R., Zhang W., Abbas Z., Guo F., Gwiazdzinski L. 2022. Spatiotemporal change analysis and prediction of future land use and land cover changes using QGIS MOLUSCE plugin and remote sensing big data: a case study of Linyi, China. *Land*, 11(3): 419. DOI: 10.3390/land11030419

Otmane T., Maachou H.M., Yousfi B. 2023. Émergence des nouvelles centralités à Oran en Algérie entre métropolisation et circulation marchande mondialisée. *Suds*, 287(1) : 53-89.

Parker D., Mitchell J.K. 1995. Editorial: Disaster vulnerability of megacities: Anexpanding problem that requires rethinking and innovative responses. *GeoJournal* 37(3): 295-301.

Peláez J.A., Hamdache M., Casado C.L. 2006. Seismic hazard in terms of spectral accelerations and uniform hazard spectra in Northern Algeria. *Pure and applied geophysics* 163: 119-135. DOI: 10.1007/s00024-005-0011-0

Pontius G.R., Malanson J. 2005. Comparison of the structure and accuracy of two land change models. *International Journal of Geographical Information Science* 19(2): 243-265. DOI: 10.1080/13658810410001713434

Pontius R.G., Boersma W., Castella J.C., Clarke K., de Nijs T., Dietzel C., Verburg P.H. 2008. Comparing the input, output, and validation maps for several models of land change. *The annals of regional science* 42: 11-37. DOI: 10.1007/s00168-007-0138-2

Puyravaud J.P. 2003. Standardizing the calculation of the annual rate of deforestation. *Forest ecology and management* 177(1-3): 593-596. DOI: 10.1016/S0378-1127(02)00335-3

Rahal F., Rezak S., Benabadji N. 2021. Influence de la pandémie du COVID-19 sur la pollution par le dioxyde d'azote dans la ville d'Oran, Algérie. *Algerian Journal of Health Sciences* 3(2): 52-57.

Rahal F., Hadjou Z., Blond N., Aguejdad R. 2018. Croissance urbaine, mobilité et émissions de polluants atmosphériques dans la région d'Oran, Algérie. Cybergeo. *European Journal of Geography*. DOI: 10.4000/cybergeo.29111

Rahman M.T.U., Esha E.J. 2022. Prediction of land cover change based on CA-ANN model to assess its local impacts on Bagerhat, southwestern coastal Bangladesh. *Geocarto International* 37(9): 2604-2626. DOI: 10.1080/10106049.2020.1831621

Rodriguez-Galiano V.F., Ghimire B., Rogan J., Chica-Olmo M., Rigol-Sanchez J.P. 2012. An assessment of the effectiveness of a random forest classifier for land-cover classification. *ISPRS journal of photo-grammetry and remote sensing* 67: 93-104. DOI: 10.1016/j.isprsjprs.2011.11.002

Roy D.P., Wulder M.A., Loveland T.R., Woodcock C.E., Allen R.G., Anderson M.C., Zhu Z. 2014. Landsat-8: Science and product vision for terrestrial global change research. *Remote Sensing of Environment* 145: 154--172. DOI: 10.1016/j.rse.2014.02.001

Shivappa Masalvad S., Patil C., Pravalika A., Katageri B., Bekal P., Patil P., Sakare P.K. 2024. Application of geospatial technology for the land use/land cover change assess-ment and future change predictions using CA Markov chain model. *Environment, Development and Sustainability* 26(10) : 24817-24842. DOI: 10.1007/s10668-023-03657-4

Song X.P. 2023. The future of global land change monitoring. *International Journal of Digital Earth* 16(1): 2279-2300. DOI: 10.1080/17538947.2023.2224586

Sun Z., Xu R., Du W., Wang L., Lu D. 2019. High-resolution urban land mapping in China from sentinel 1A/2 imagery based on Google Earth Engine. *Remote Sensing* 11(7): 752. DOI: 10.3390/rs11070752

Trache S.M., Khelifi M. 2020. Périurbanisation et décroissance démographique de la ville centre: l'exemple d'Oran (Algérie). *Cahiers de géographie du Québec* 64(181): 169-189. DOI: 10.7202/1090226ar

Turner B.L., Lambin E.F., Reenberg A. 2007. The emergence of land change science for global environmental change and sustainability. *Proceedings of the National Academy of Sciences* 104(52): 20666-20671. DOI: 10.1073/pnas.0704119104

USGS. 2025. US Geological Survey EarthExplorer. Online: https://earthexplorer.usgs.gov (last access: 11.02.2025).

Verburg P.H., Erb K.H., Mertz O., Espindola G. 2013. Land System Science: between global challenges and local realities. *Current opinion in environmental sustainability* 5(5): 433-437. DOI: 10.1016/j.cosust.2013.08.001

Verburg P.H., Schot P.P., Dijst M.J., Veldkamp A. 2004. Land use change modelling: current practice and research priorities. *GeoJournal* 61: 309-324. DOI: 10.1007/s10708-004-4946-y

Wald D.J., Allen T.I. 2007. Topographic slope as a proxy for seismic site conditions and amplification. *Bulletin of the Seismological Society of America* 97: 1379-1395. DOI: 10.1785/0120060267.

Wenzel F., Bendimerad F., Sinha R. 2007. Megacities – megarisks. *Natural Hazards* 42: 481-491. DOI:10.1007/s11069-006-9073-2.

Yang K., Hou H., Li Y., Chen Y., Wang L., Wang P., Hu T. 2022. Future urban waterlogging simulation based on LULC forecast model: A case study in Haining City, China. *Sustainable Cities and Society* 87: 104167. DOI: 10.1016/j.scs.2022.104167

Yelles-Chaouche A.K., Boudiaf A., Djellit H., Bracene R. 2006. Active tectonics in northern Algeria. *Comptes rendus Géoscience* 338 (1--2): 126-139. DOI: 10.1016/j.crte.2005.11.002